

Nuclear shapes in covariant density functionals theory: recent results

Anatoli Afanasjev

Mississippi State University

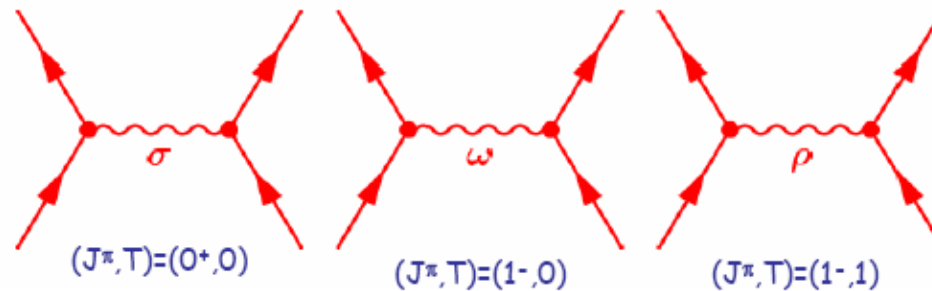
1. Motivation
2. Global analysis of octupole deformation with an assessment of theoretical uncertainties.
3. The competition of oblate and spherical deformations in superheavy nuclei
4. Extreme deformations and clusterization in the $A \sim 40$ $N \sim Z$ nuclei
5. Conclusions

In collaboration with

S. Abgemava, D. Ray (MSU), P. Ring (TU Munich)
and T. Nakatsukasa (Tsukuba U)

Covariant density functional theory (CDFT)

The nucleons interact via the exchange of effective mesons →
→ **effective Lagrangian**



Long-range
attractive
scalar field

Short-range
repulsive vector
field

Isovector
field

$$E_{\text{RMF}}[\hat{\rho}, \phi_m] = \text{Tr}[(\alpha p + \beta m)\hat{\rho}] \pm \int \left[\frac{1}{2}(\nabla \phi_m)^2 + U(\phi_m) \right] d^3r + \text{Tr}[(\Gamma_m \phi_m)\hat{\rho}]$$

density matrix $\hat{\rho}$ $\phi_m \equiv \{\sigma, \omega^\mu, \vec{\rho}^\mu, A^\mu\}$ - meson fields

$$\hat{h} = \frac{\delta E}{\delta \hat{\rho}}$$

**Mean
field**

$$\hat{h}|\varphi_i\rangle = \varepsilon_i|\varphi_i\rangle$$

Eigenfunctions

Motivation: few words about global studies and assesment of theoretical uncertainties

Global performance

Ground state observables: S.E.Agbemava, AA, D.Ray and P.Ring, PRC 89, 054320 (2014), AA and S. Abgemava PRC 93, 054310 (2016)

Neutron drip lines and sources of their uncertainties:

PLB 726, 680 (2013), PRC 89, 054320 (2014), PRC 91, 014324 (2015)

Systematic studies in local regions (mostly actinides)

Accuracy of the description of deformed one-quasiparticle states

AA and S.Shawaqfeh, PLB 706 (2011) 177

Fission barriers in actinides and SHE

actinides: H. Abusara, AA and P. Ring, PRC 82, 044303 (2010)

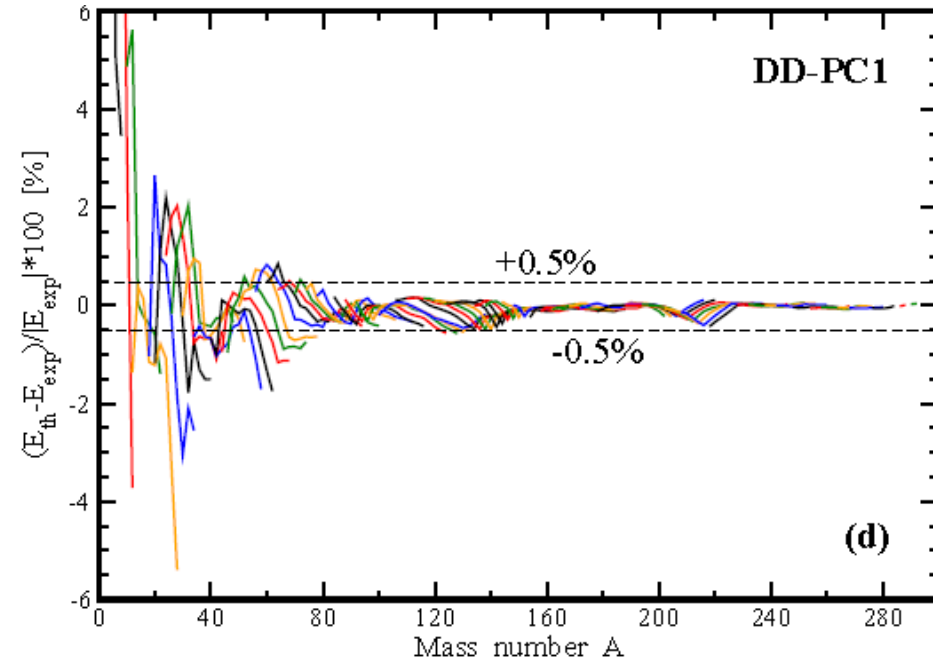
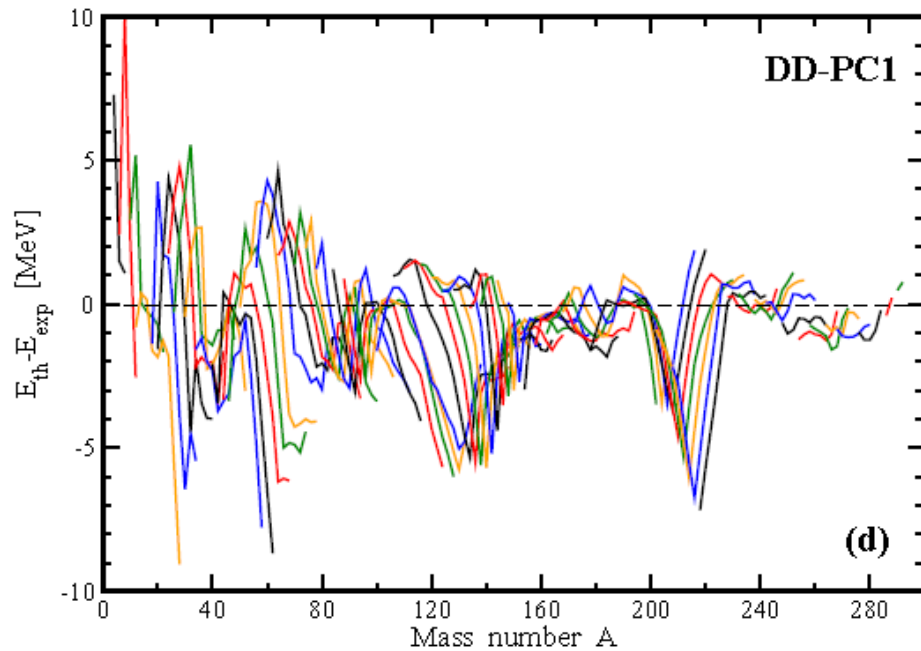
superheavies: H. Abusara, AA and P. Ring, PRC 85, 024314 (2012)

Pairing and rotational properties of even-even of odd-mass actinides

AA and O.Abdurazakov, PRC 88, 014320 (2013),

AA, Phys. Scr. 89 (2014) 054001

Systematic errors in the RHB description of masses



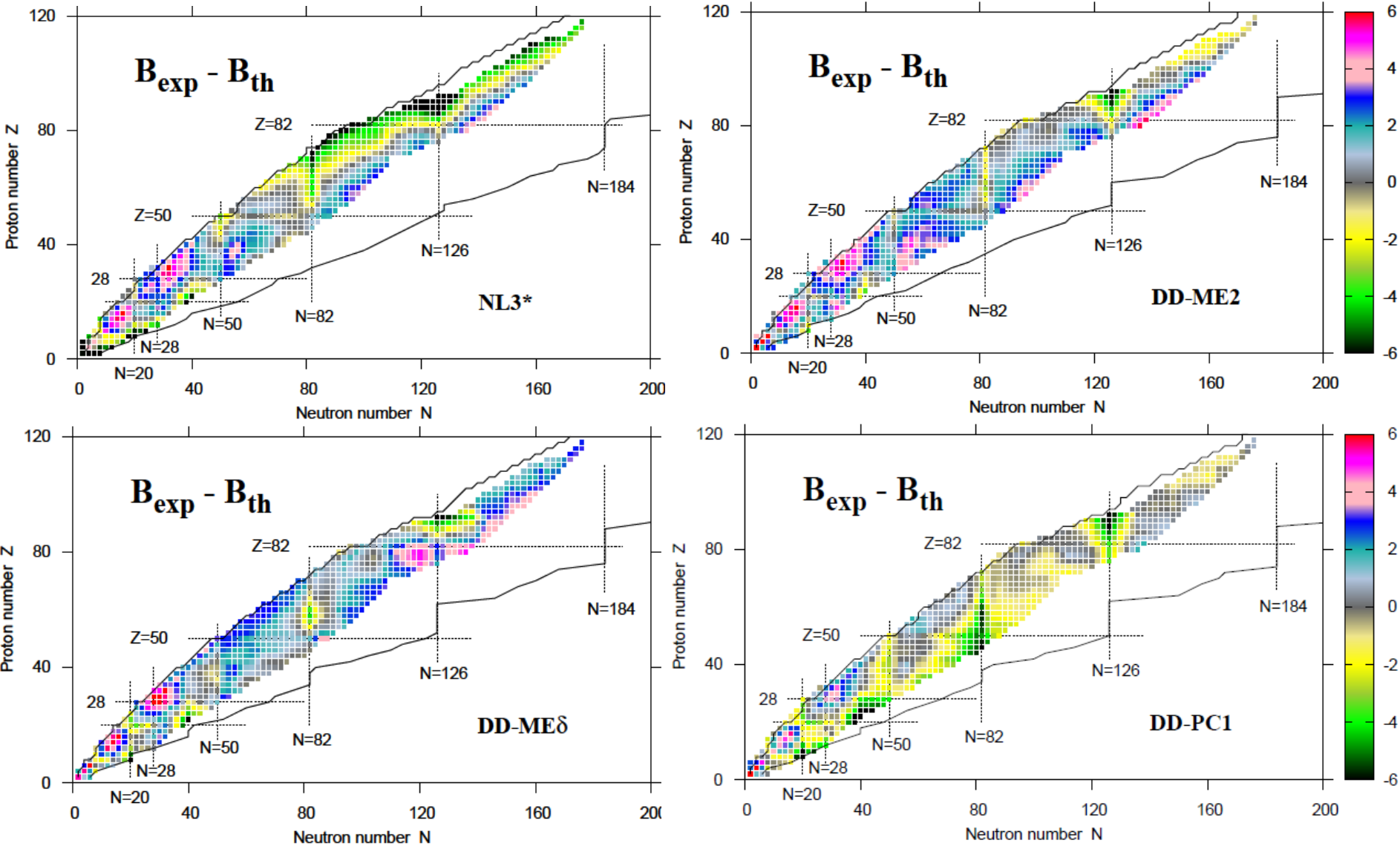
EDF	measured	measured+estimated		
	ΔE_{rms}	ΔE_{rms}	$\Delta(S_{2n})_{rms}$	$\Delta(S_{2p})_{rms}$
NL3*	2.96	3.00	1.23	1.29
DD-ME2	2.39	2.45	1.05	0.95
DD-ME δ	2.29	2.40	1.09	1.09
DD-PC1	2.01	2.15	1.16	1.03

Uncertainties in radii

CEDF	Δr_{ch}^{rms} [fm]
NL3*	0.0283
DD-ME2	0.0230
DD-MEd	0.0329
DD-PC1	0.0253

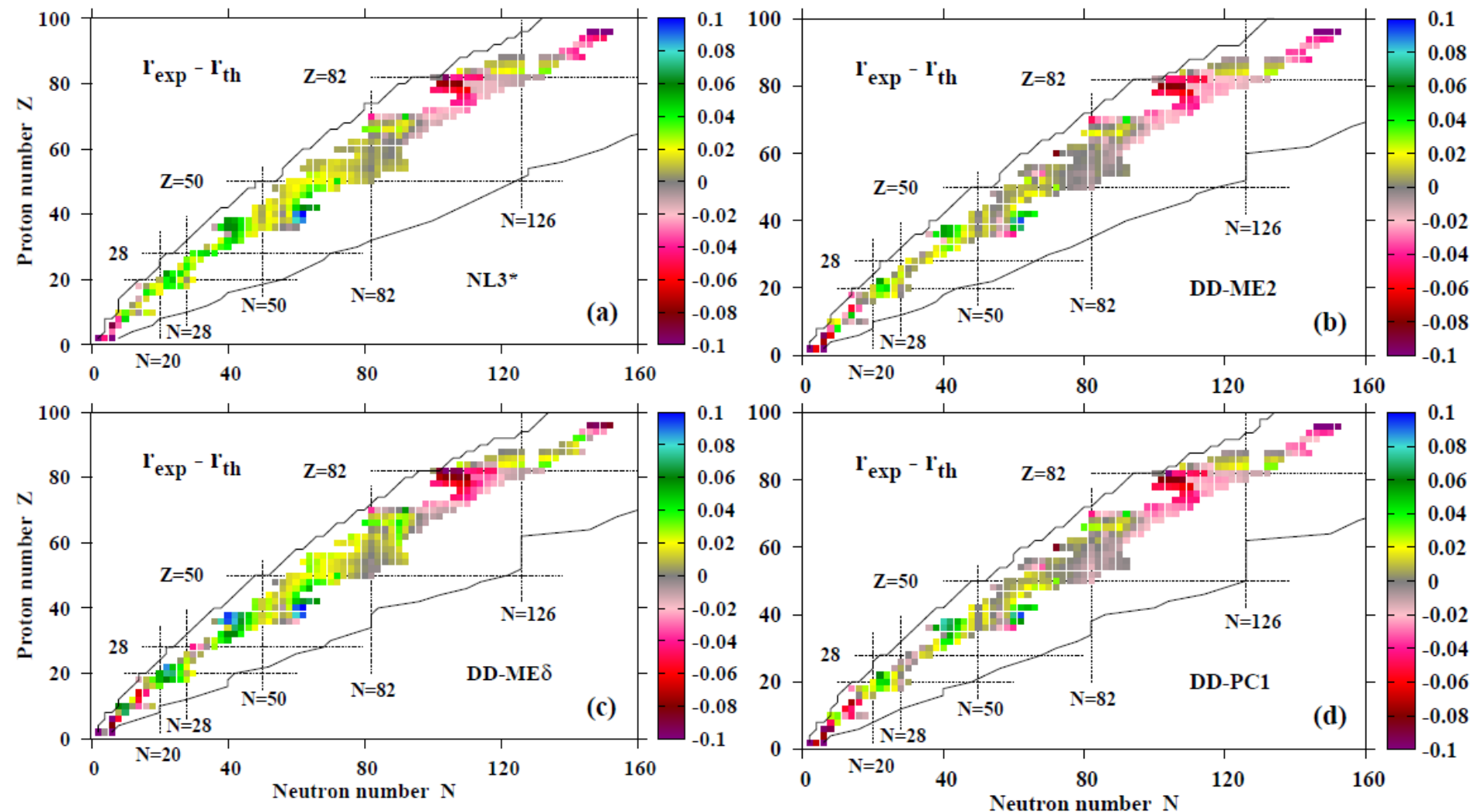
S. Agbemava, AA, D, Ray, P.Ring, PRC **89**, 054320 (2014) includes complete DD-PC1 mass table as supplement

Masses: the deviations between theory and experiment



The residuals are non-statistical in nature \rightarrow the difficulty in the estimation of systematic errors in unknown regions

Systematic errors in the description of charge radii



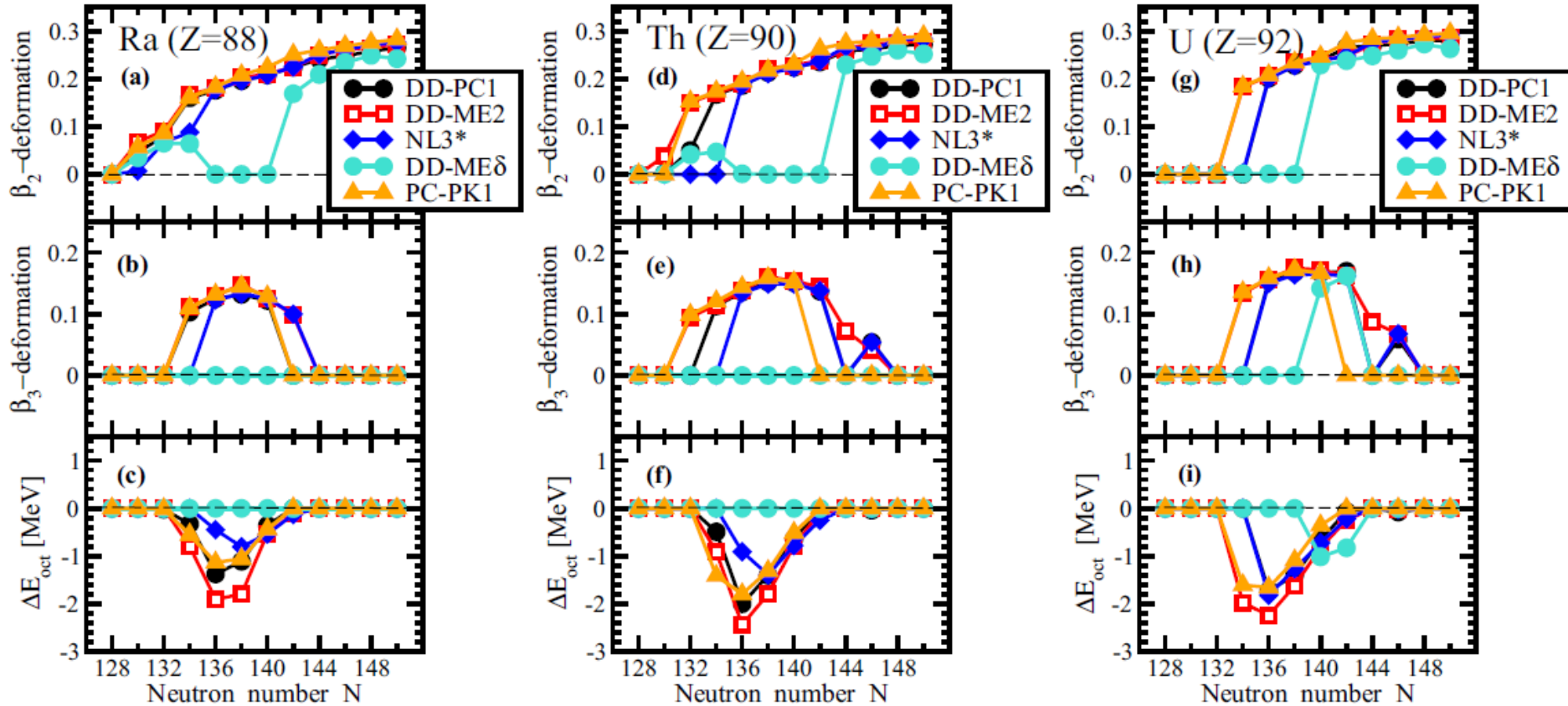
Charge radii – rather well described in all functionals
- very little difference between CEDFs

Global analysis of octupole deformation with an assessment of theoretical uncertainties.

according to S. Agbemava, AA and P. Ring, PRC 93, 044304 (2015)

RHB calculations with separable pairing

Octupole deformation in Ra-Th-U isotopes and related theoretical uncertainties in predictions

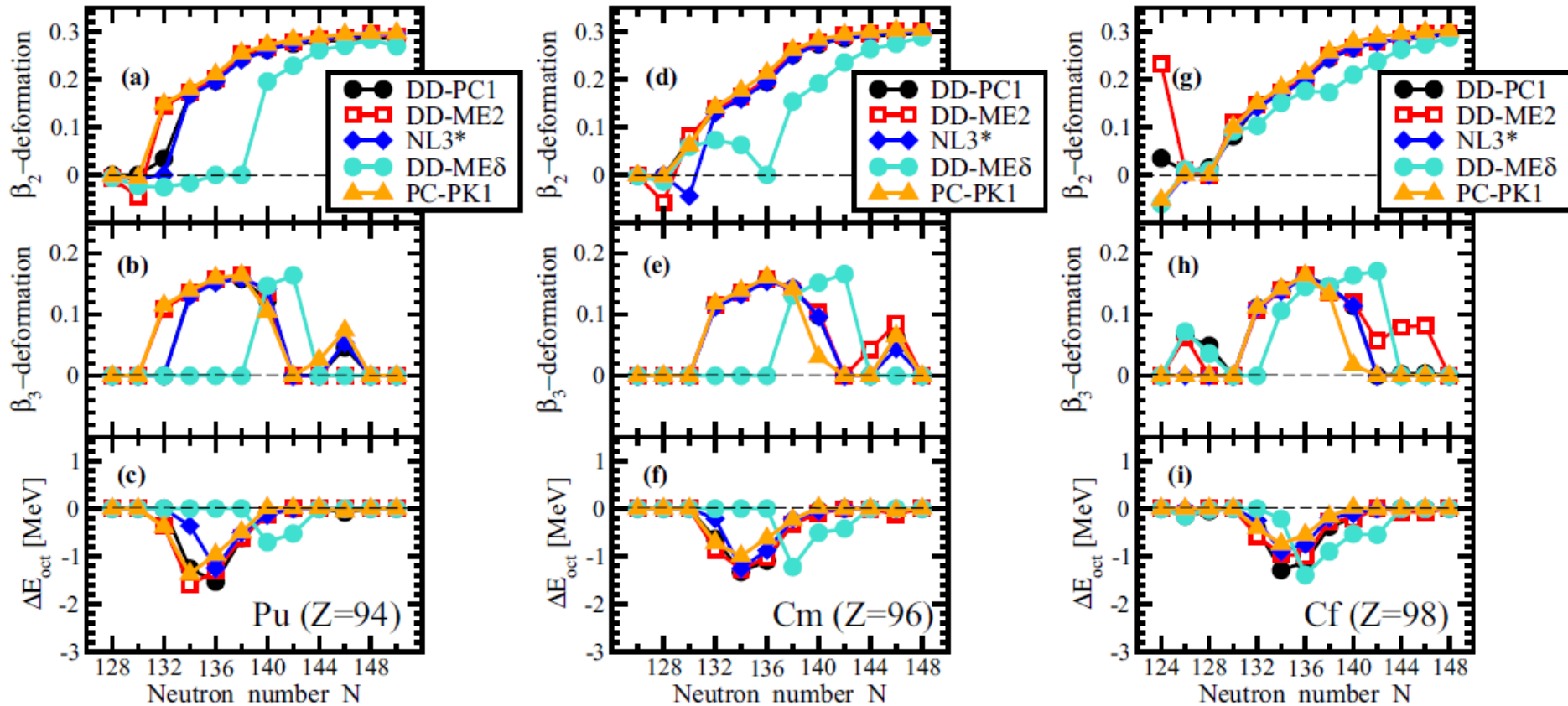


$$\Delta E_{\text{oct}} = E^{\text{oct}}(\beta_2, \beta_3) - E^{\text{quad}}(\beta'_2, \beta'_3 = 0)$$

- $|\Delta E_{\text{oct}}|$ - the gain of binding due to octupole deformation
- indicator of stability of the octupole deformed shapes (small – octupole soft, large – static octupole deformation)

The maximum gain in binding due to octupole deformation takes place at $N \sim 136$ in the Ra, Th and U isotopes which agrees with experimental data.

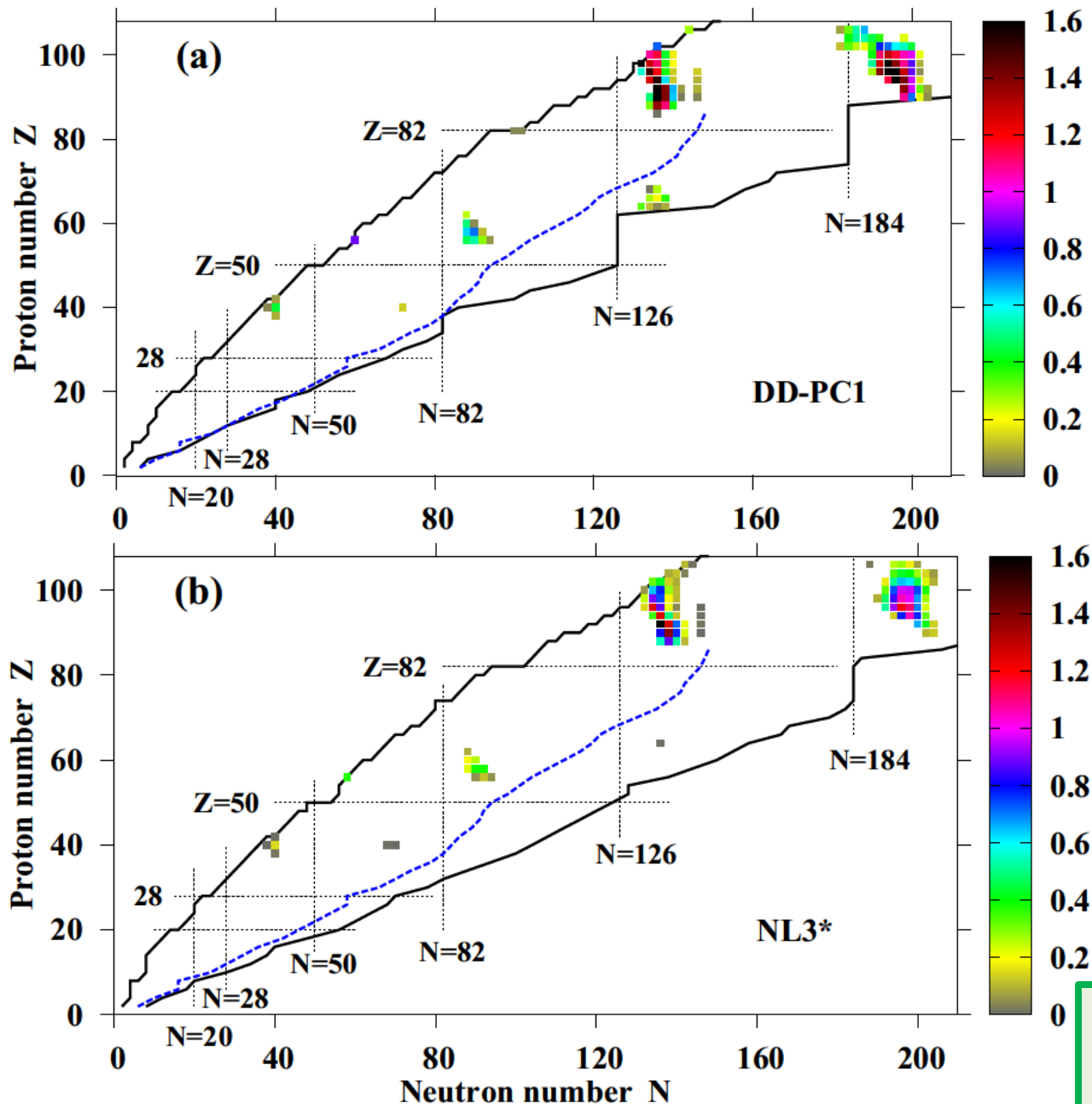
Octupole deformation in Pu-Cm-Cf isotopes and related theoretical uncertainties in predictions



There are no experimental data on octupole deformed Pu, Cm and Cf isotopes

The RHB calculations predict the weakening of the stabilization of octupole deformation with increasing Z

Global search for octupole deformed nuclei



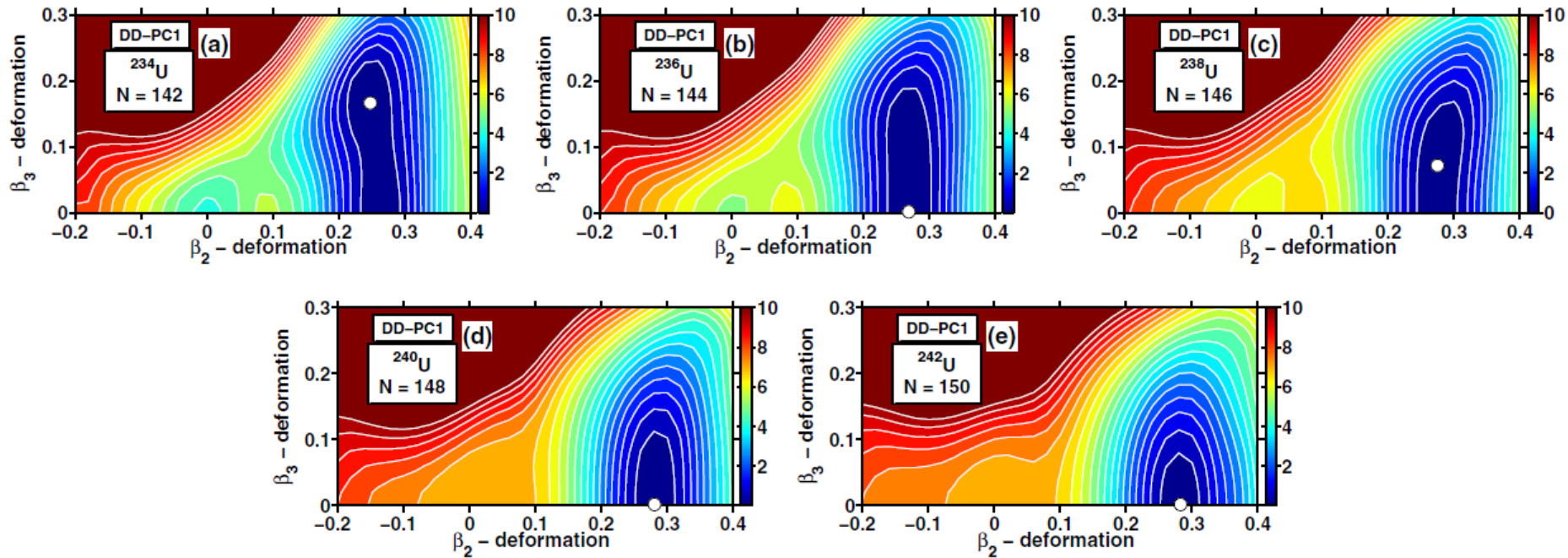
Colormap shows the gain in binding due to octupole deformation.

A new region of octupole deformation, centered around $Z \sim 98$, $N \sim 196$, has been predicted for the first time.

the interaction of the $2h_{11/2}$ and $1k_{17/2}$ neutron orbitals and of the $1i_{13/2}$ and $2f_{7/2}$ proton orbitals is responsible for it

Will impact fission recycling in neutron star mergers

How to understand these features?



1. PES of the $N \leq 146$ actinides are soft in octupole deformation. Thus, at low spin these nuclei are in octupole vibrational regime in which the CRHB+LN calculations with no octupole deformation describe well the moments of inertia. However, the transition to static octupole deformation (not taken into account in the calculations) takes at higher spin; it leads to a delay of alignment.
2. PES of the $N \geq 148$ actinides are stiff in octupole deformation. \rightarrow no transition to static octupole deformation at high spin and good description in the CRHB+LN calculations.

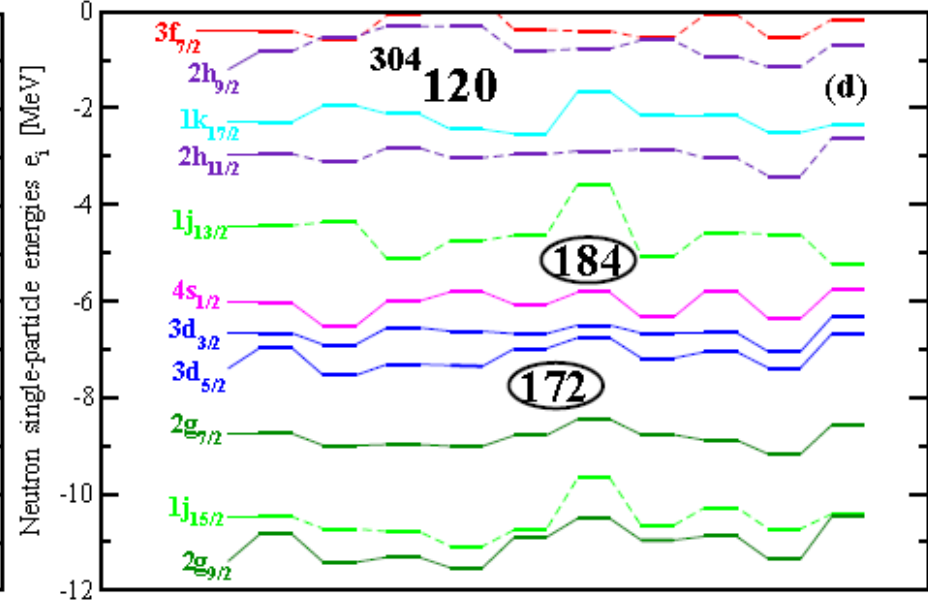
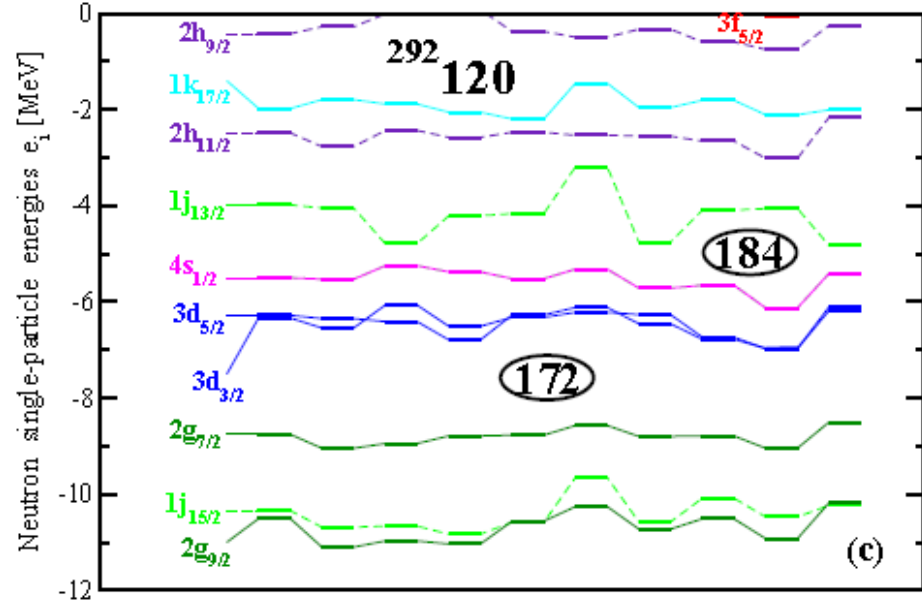
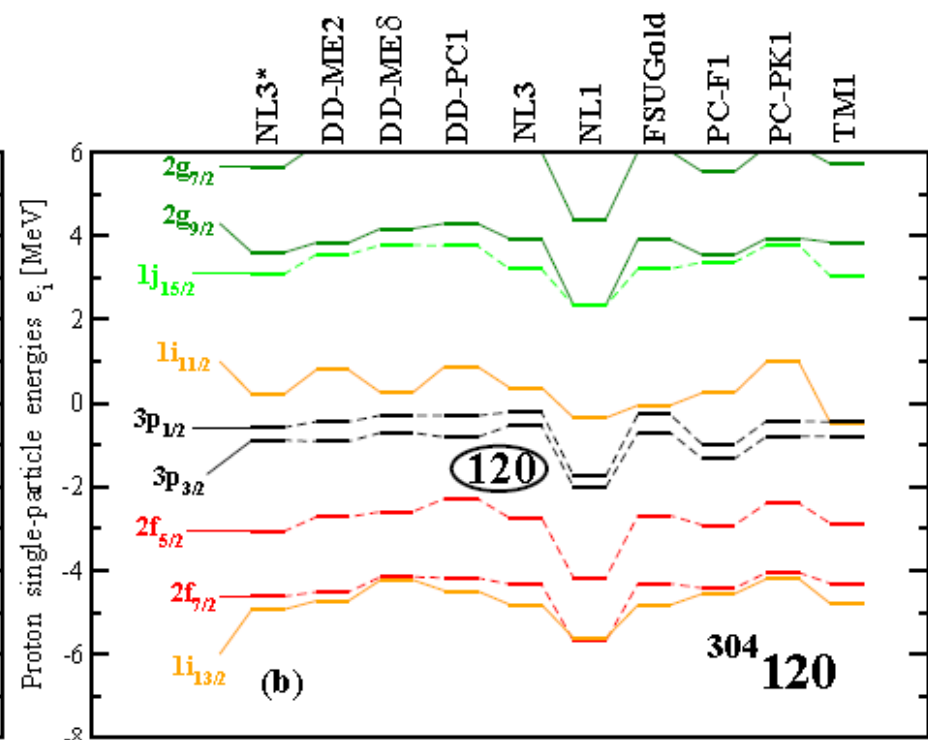
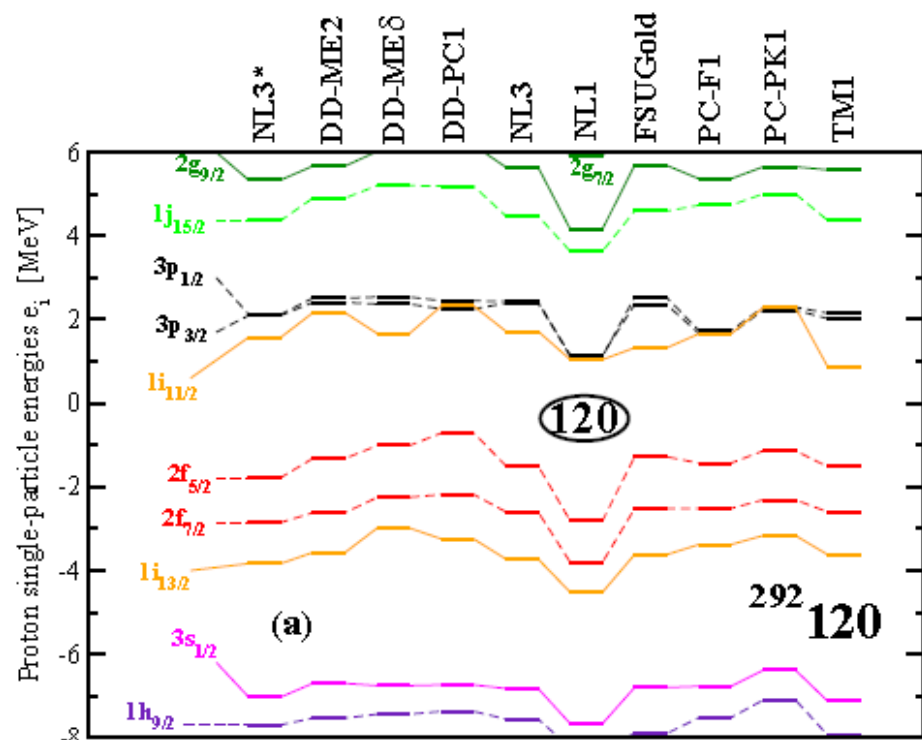
The competition of oblate and spherical deformations in superheavy nuclei

according to S. Agbemava, AA, T. Nakatsukasa, P. Ring,
PRC 92, 054310 (2015)

includes as a supplement to the manuscript

complete mass, deformation and radii table for even-even nuclei with $106 < Z < 130$ obtained with DD-PC1 and PC-PK1

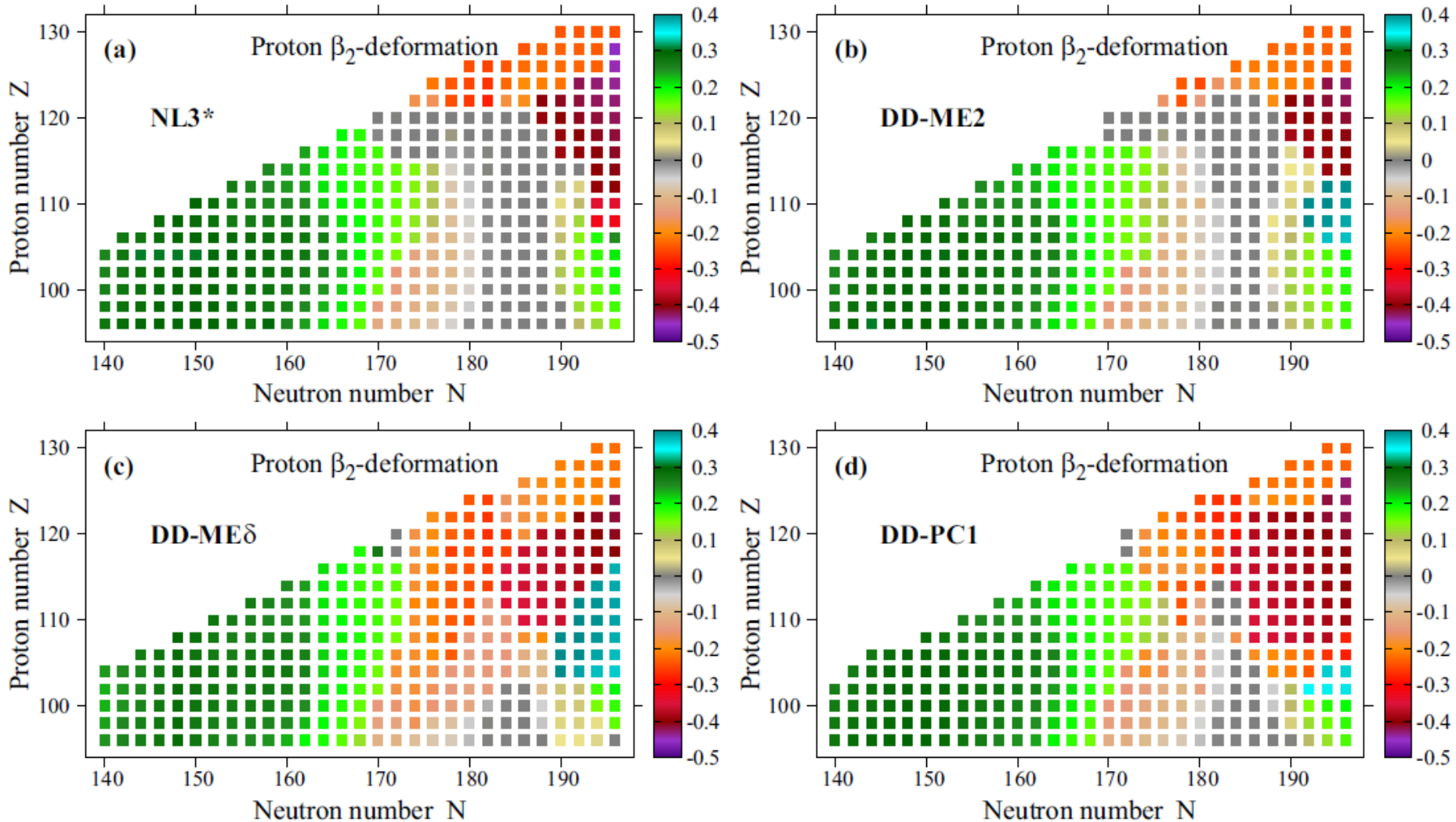
RHB calculations with separable pairing



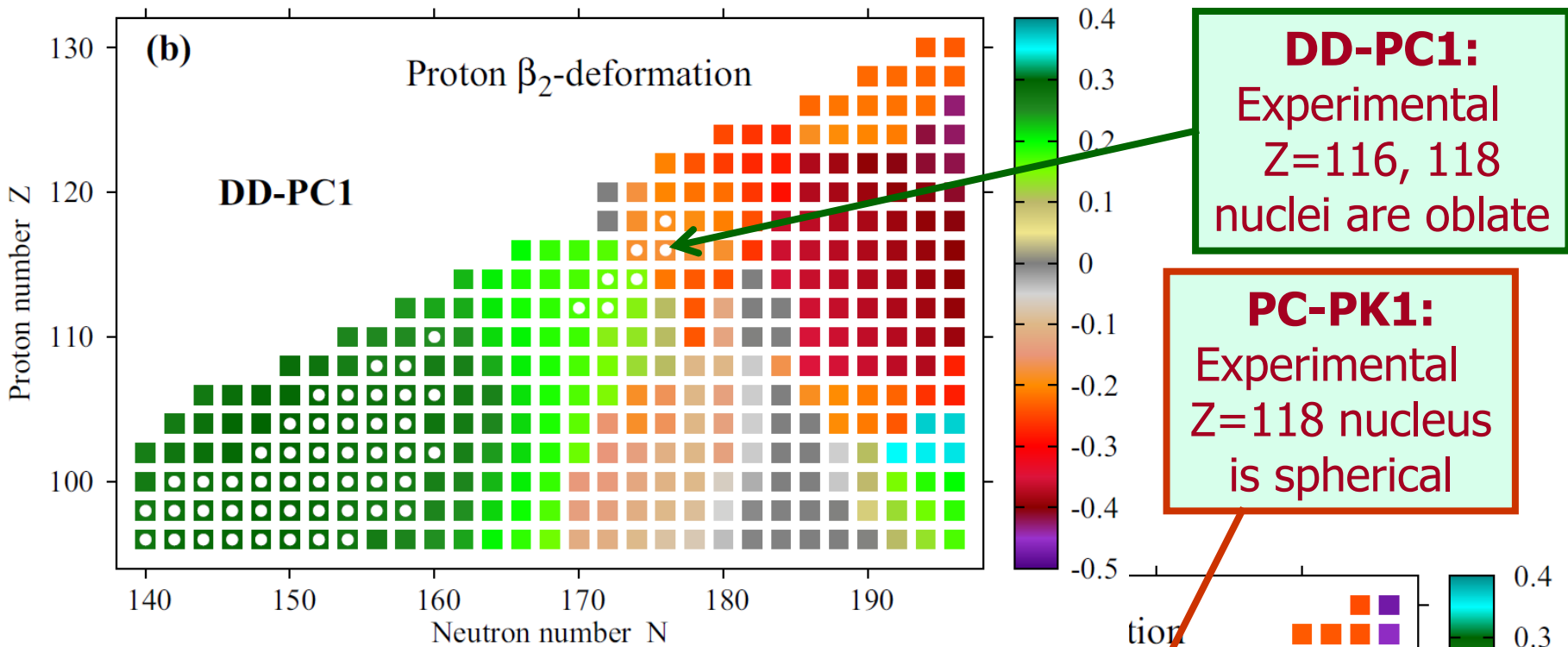
Deformation effects on shell structure

→ Very important – deformed results differ substantially from spherical ones

Unusual feature: oblate shapes above the spherical shell closures

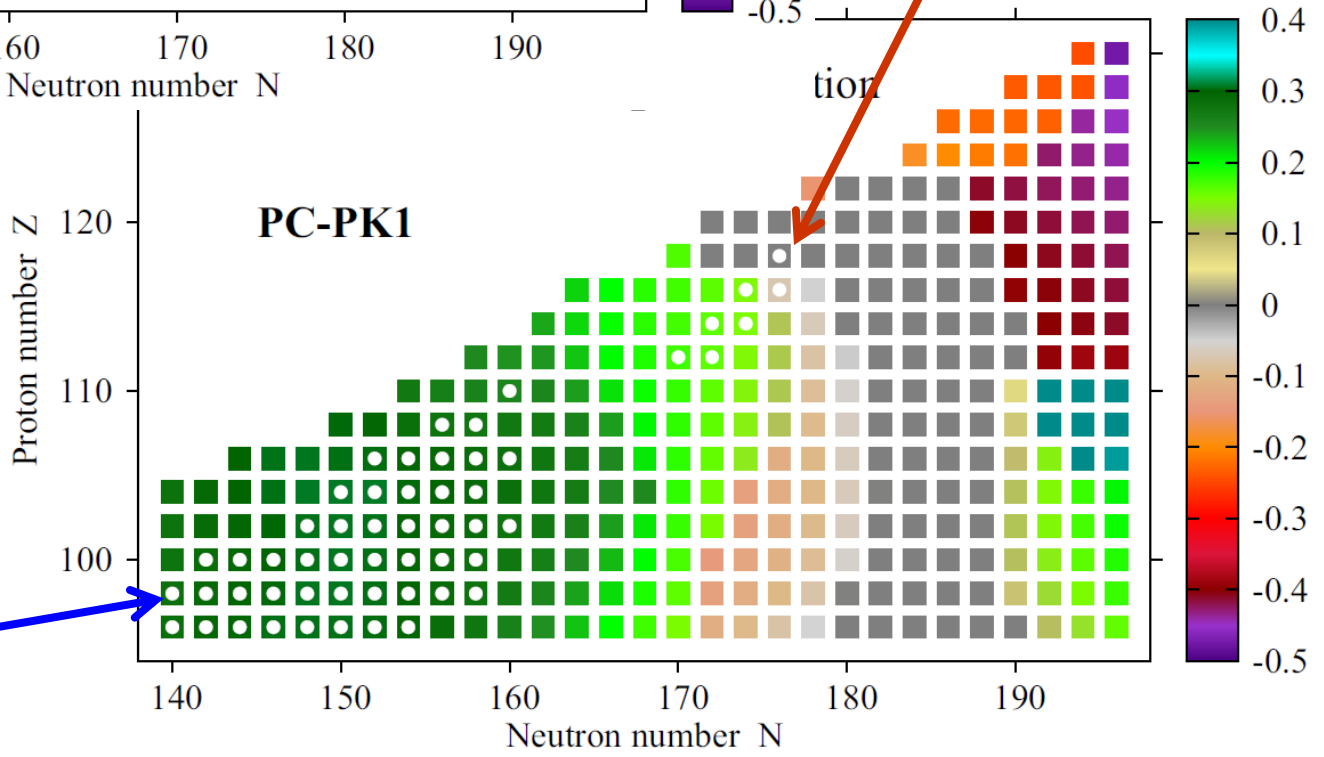


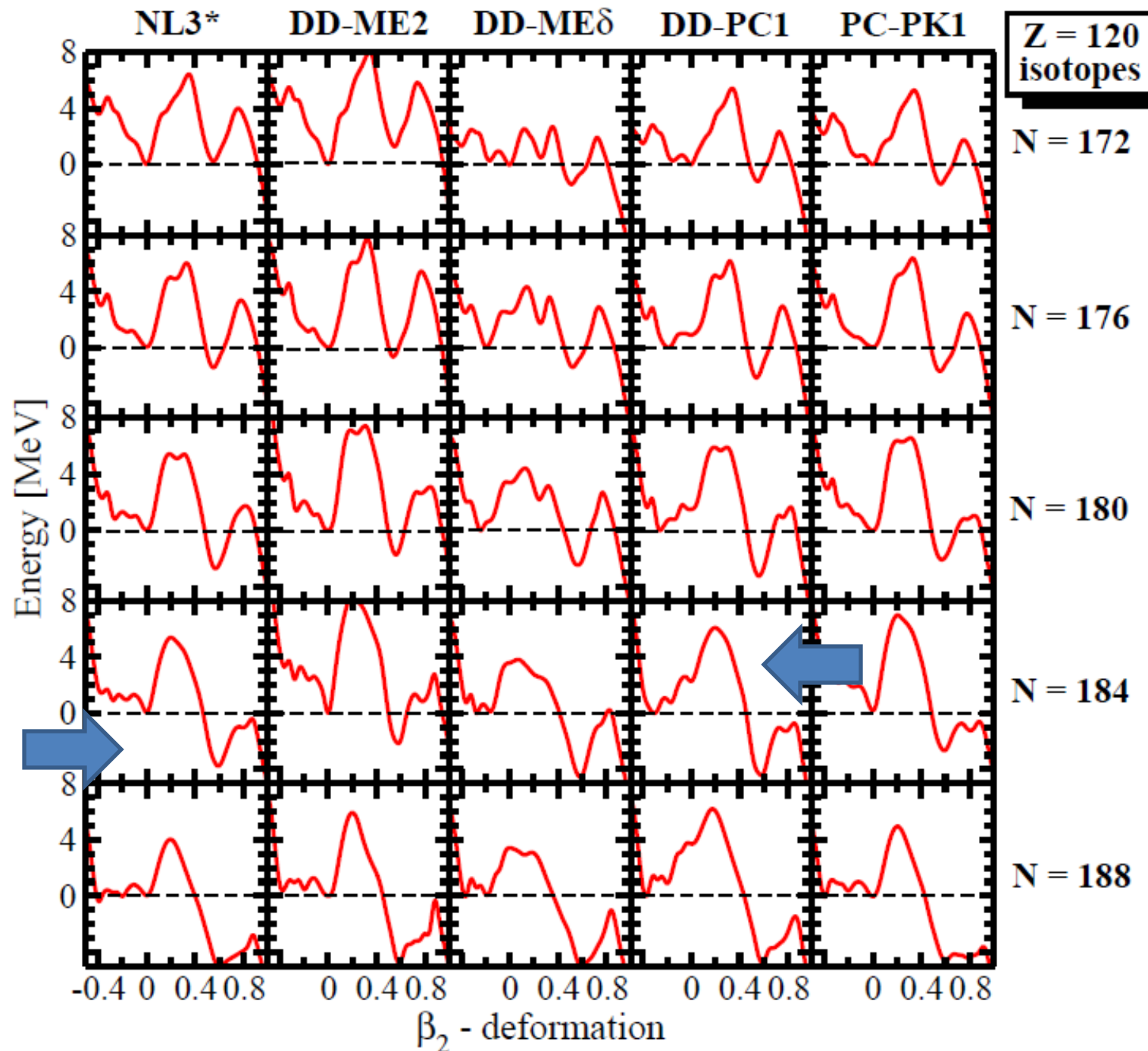
Results for PC-PK1 are very similar to the ones with NL3*



Other experimental SHE are prolate

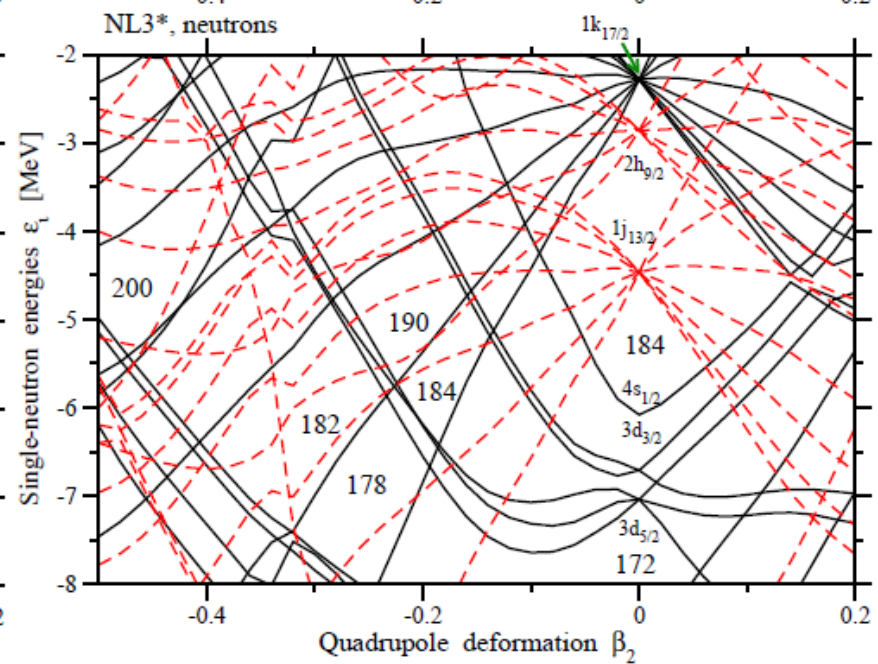
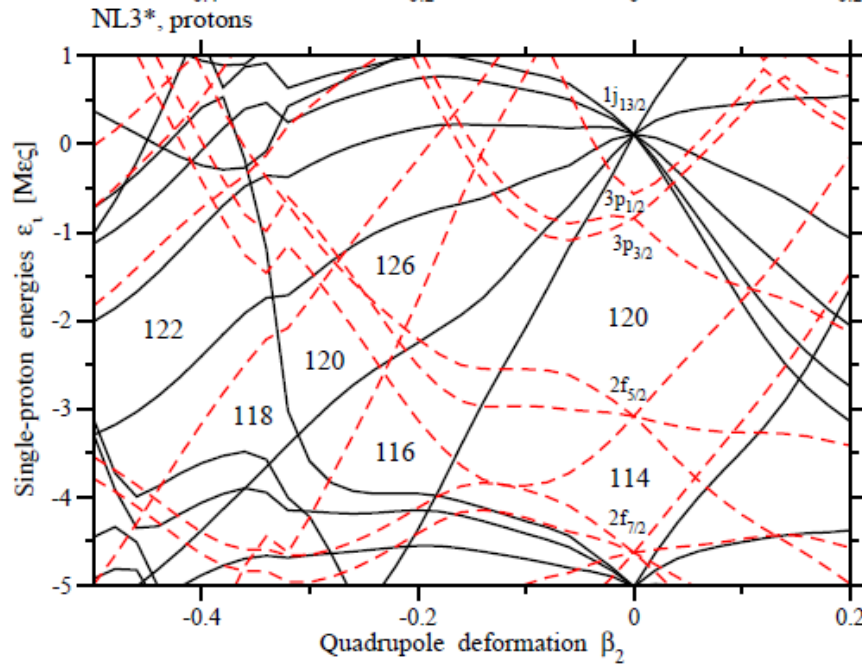
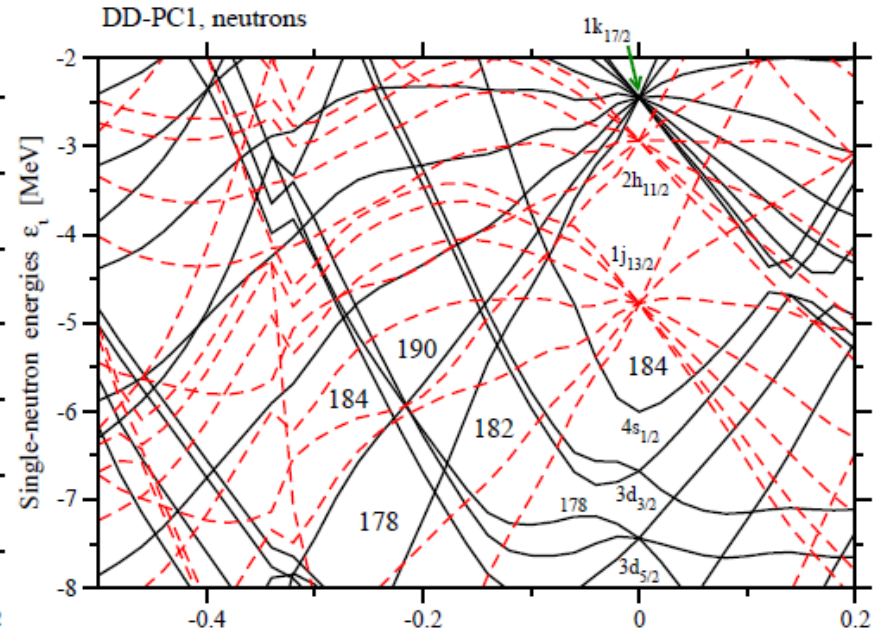
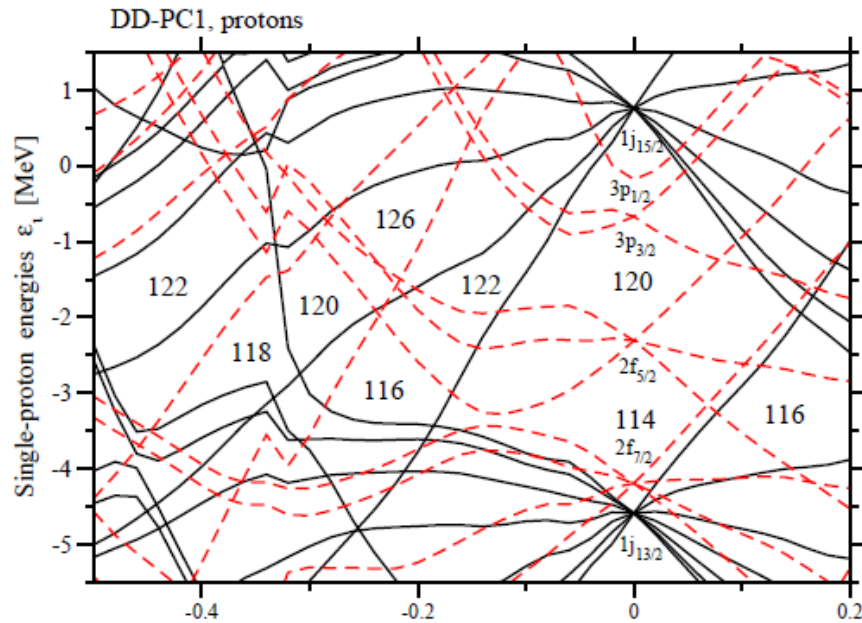
Open circles – experimentally observed nuclei



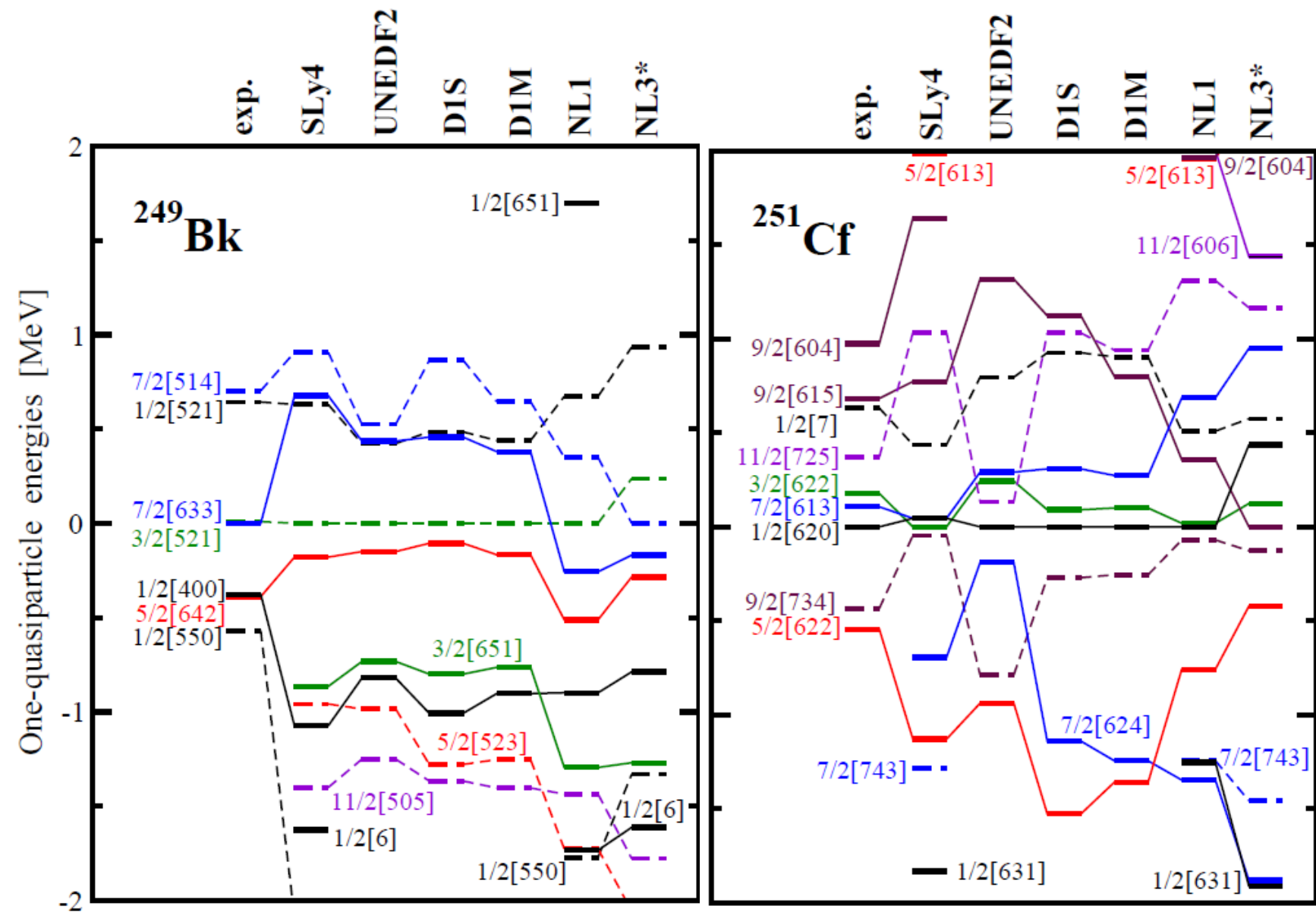


Potential energy surfaces in axially symmetric RHB calculations with separable pairing

The source of oblate shapes – the low density of s-p states



Deformed one-quasiparticle states: covariant and non-relativistic DFT description versus experiment



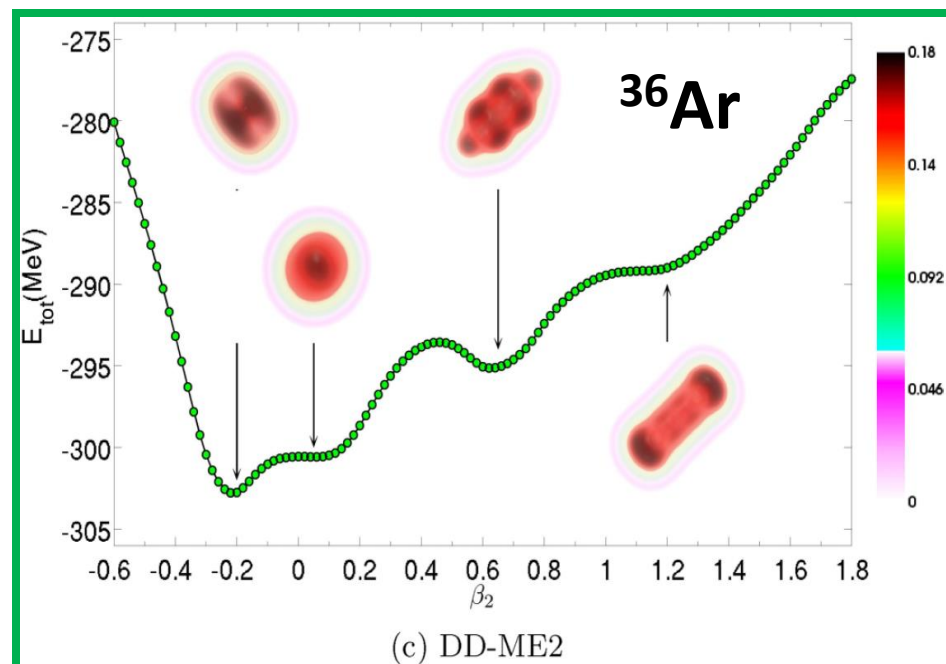
Extreme deformations and clusterization in the $A \sim 40$ $N \sim Z$ nuclei

according to D. Ray and AA, PRC 94, 014310 (2016)

CRMF calculations with no pairing

Density functional studies of cluster states in nuclei

From J.P. Ebran et al, PRC 90, 054329 (2014)



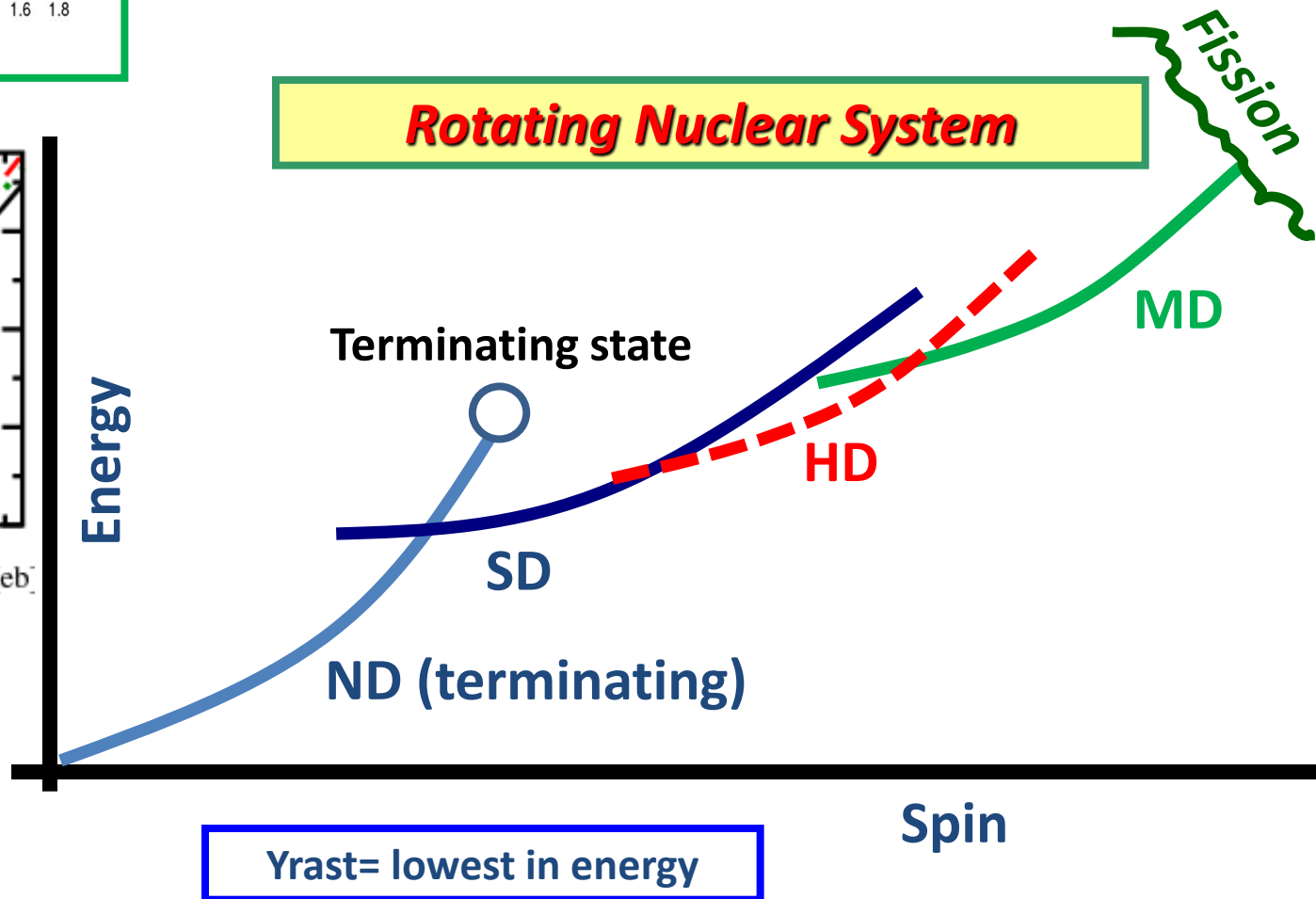
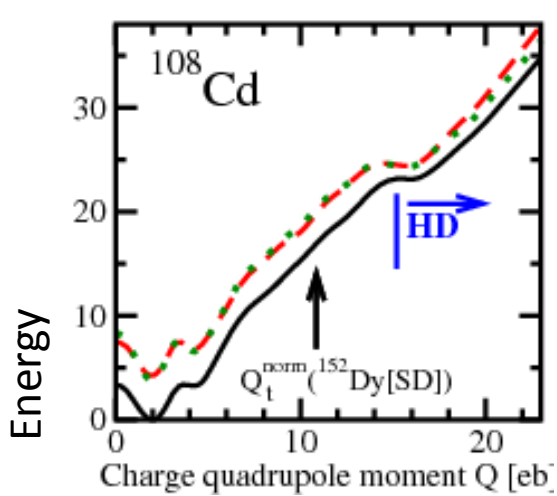
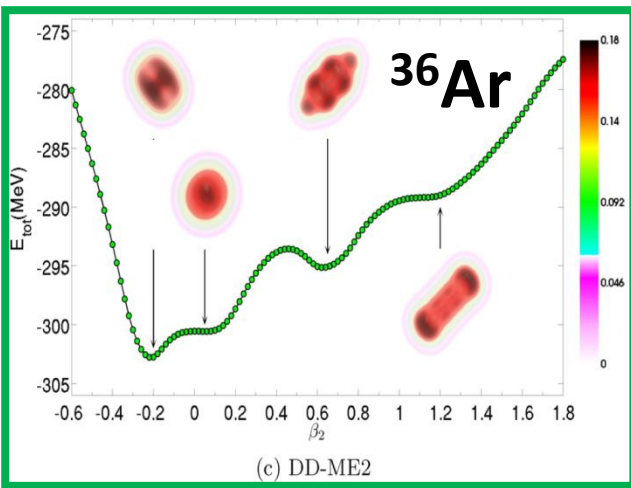
Relativistic functionals (as compared with non-relativistic ones) predict much more pronounced cluster structures
J.P.Ebran et al, Nature 487, 341 (2012)

How to observe these states in experiment?

How to observe the extreme deformation and clusterization?

$I=0$ system

Rotating Nuclear System



What is important for observation of extremely deformed structures at high spin?

1. Such structures have to be yrast (lowest in energy at given spin) or near-yrast at the spins where the feeding takes place. Otherwise, lower deformed configurations will be fed with much higher intensity.
2. Highest spins observed in experiment in even-even nuclei of the mass region of interest is $I=16$ (SD bands in ^{36}Ar and ^{40}Ca and ND band in ^{48}Cr)

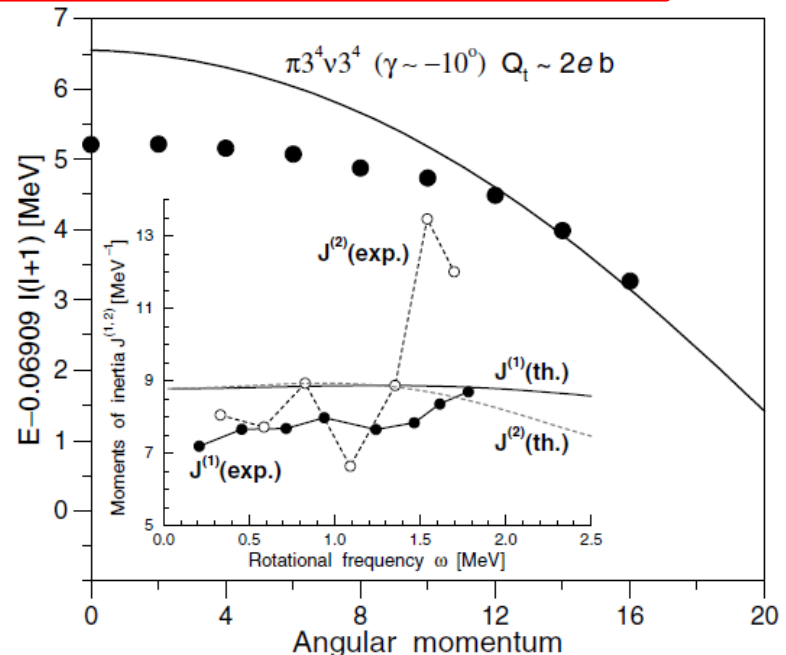
Neglect of pairing in the CRMF calculations

Quenching of pairing at high spin in deformed structures due to

- Coriolis antipairing effect
- large shell gaps
- blocking effect.

Typically above $I \sim 10$ in the mass region of interest

Pairing is very weak near the termination of rotational bands



Configuration labelling

Pairing correlations are neglected \rightarrow intrinsic structure of the configurations
Can be described by means of the dominant single-particle components of the
intruder/hyperintruder/megaintruder states occupied.

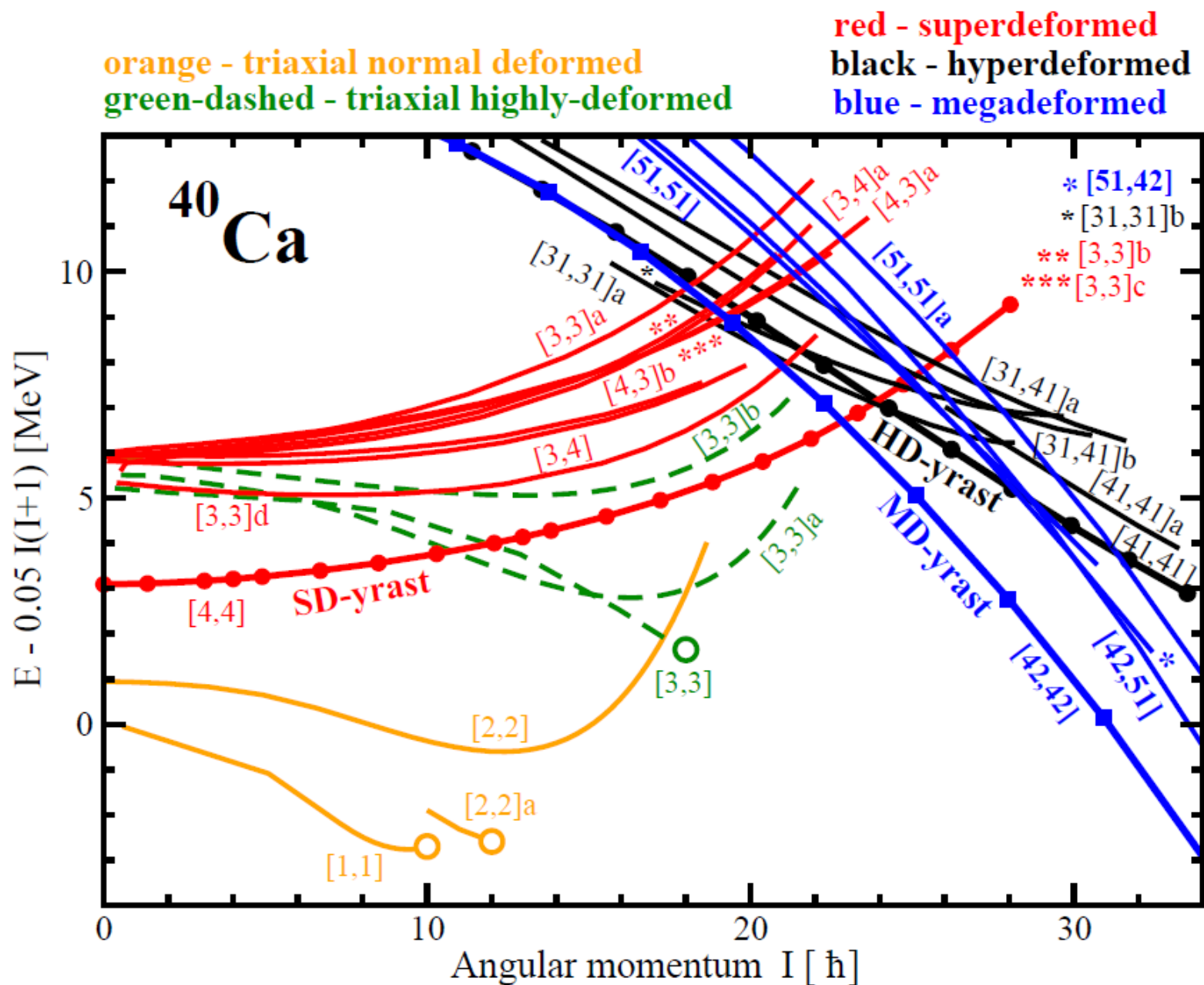
Shorthand notation $[n_1(n_2)(n_3), p_1(p_2)(p_3)]$

n_1 (p_1) - # of neutrons (protons) in the intruder N=3 orbitals

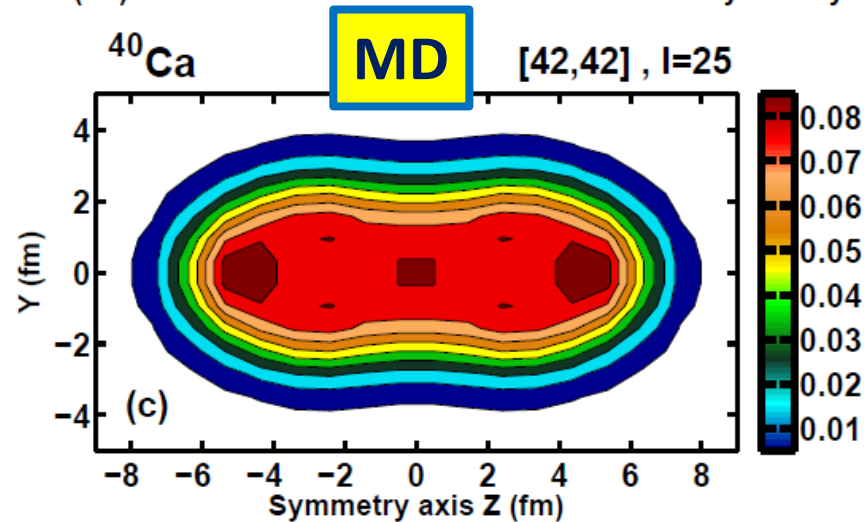
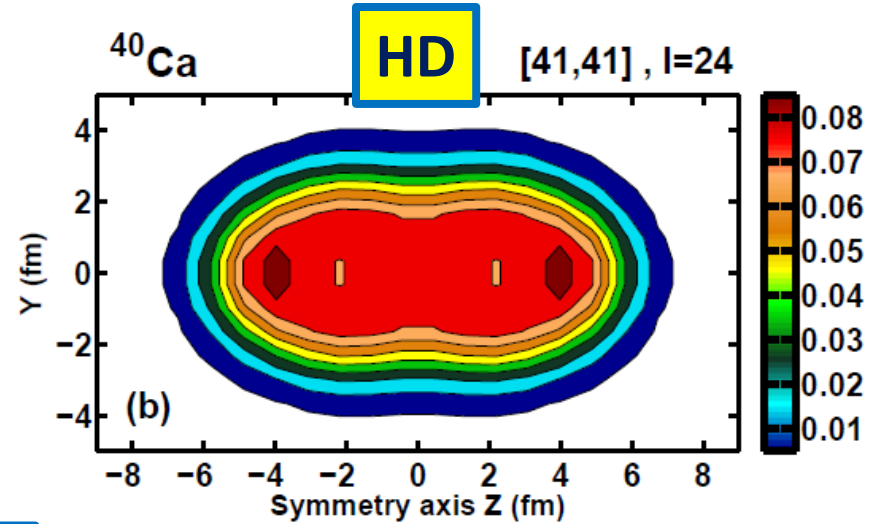
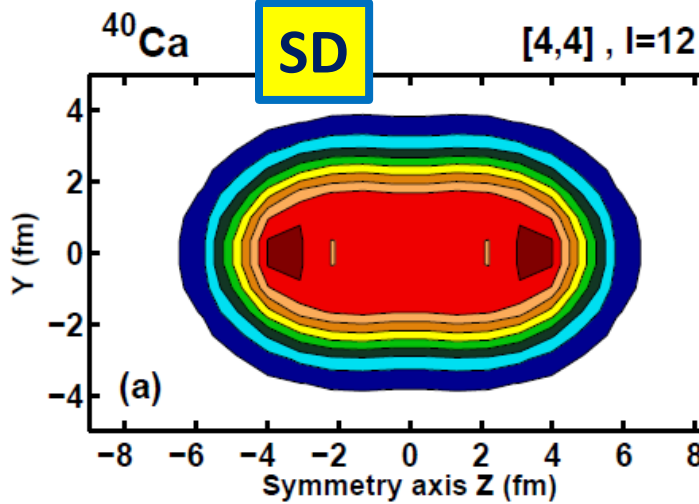
n_2 (p_2) - # of neutrons (protons) in the hyperintruder N=4 orbitals

n_3 (p_3) - # of neutrons (protons) in the megaintruder N=5 orbitals

High-spin structure of the ^{40}Ca nucleus



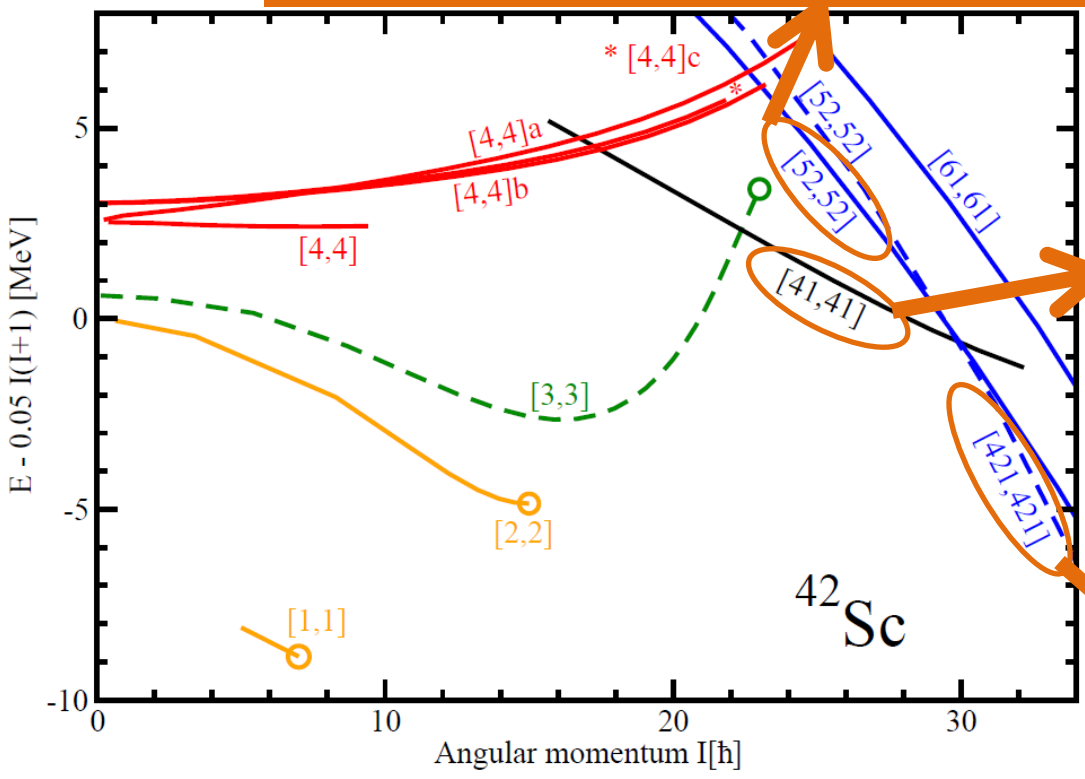
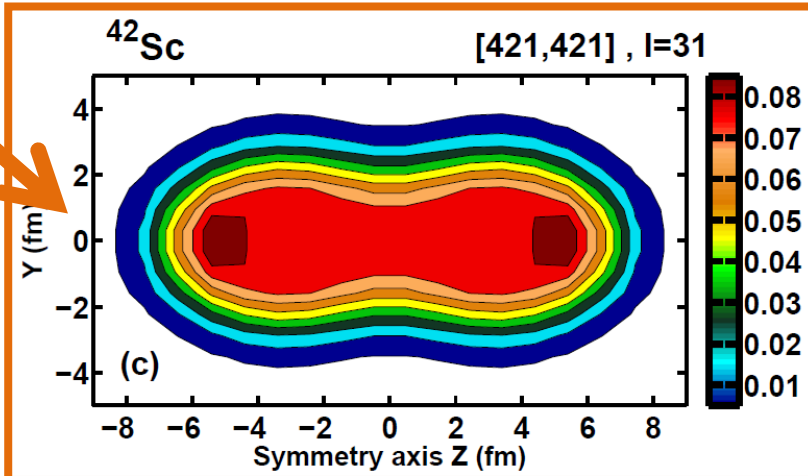
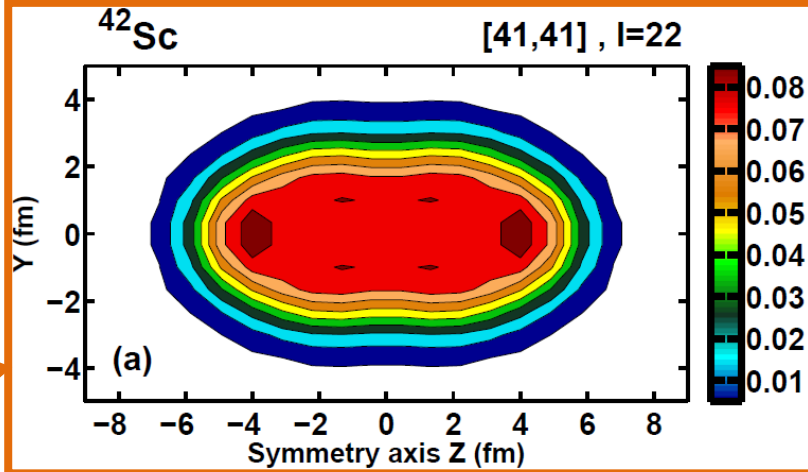
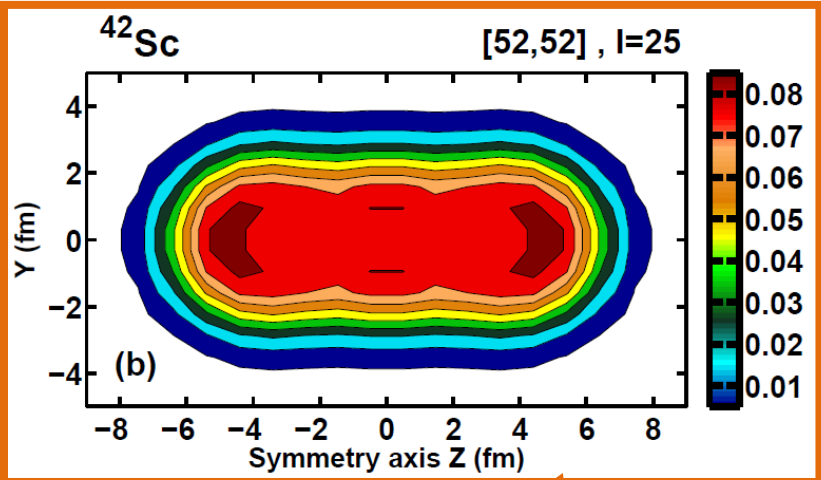
Density distribution: enhancement of clusterization with deformation



$^{12}\text{C}+^{16}\text{O}+^{12}\text{C}$?

$^{20}\text{Ne}+^{20}\text{Ne}$?

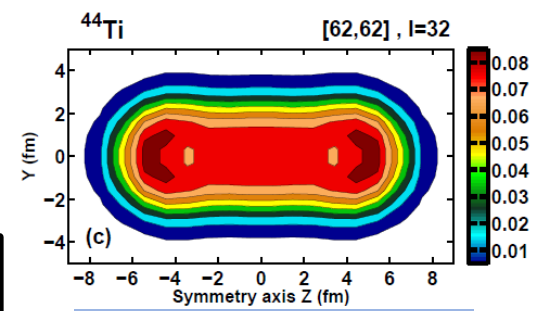
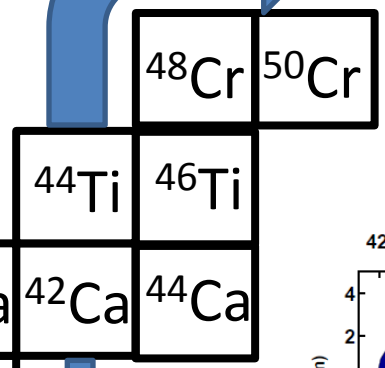
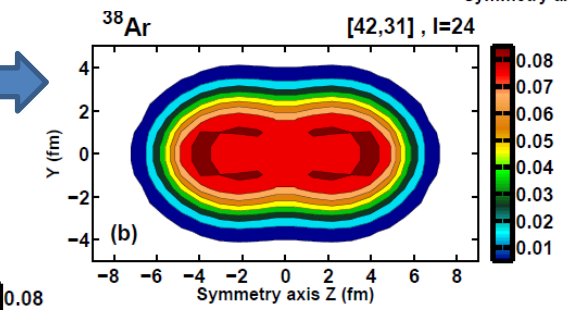
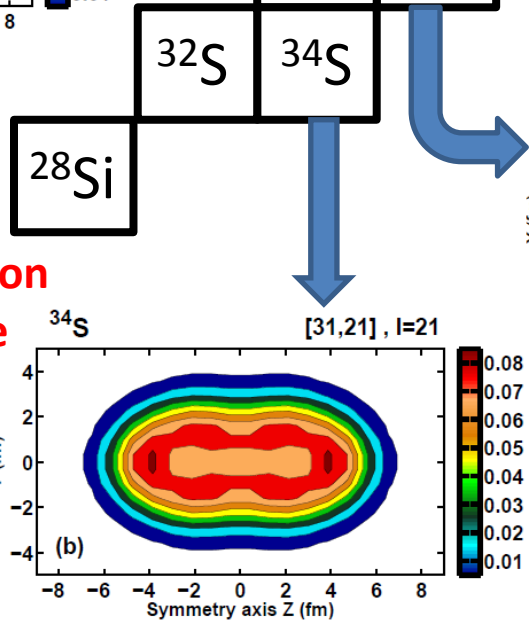
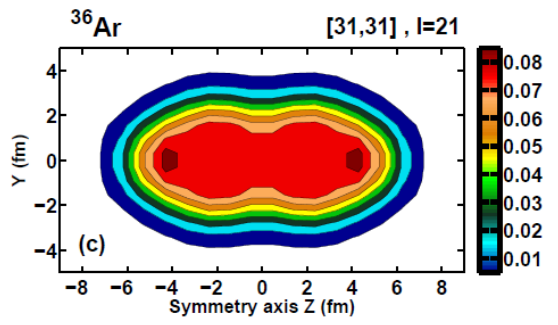
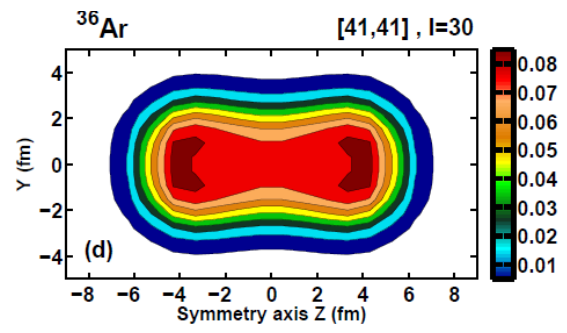
High-spin structure of the $N=Z=21$ ^{42}Sc nucleus



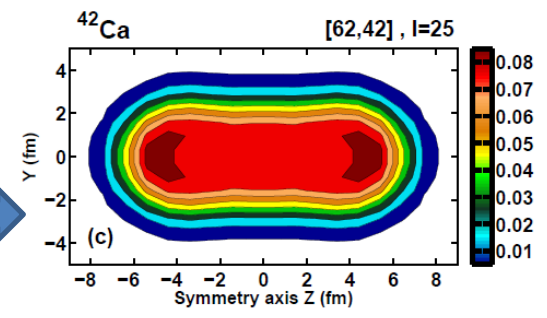
Systematics of interesting configurations

Rod-shape structures

Nuclear molecules



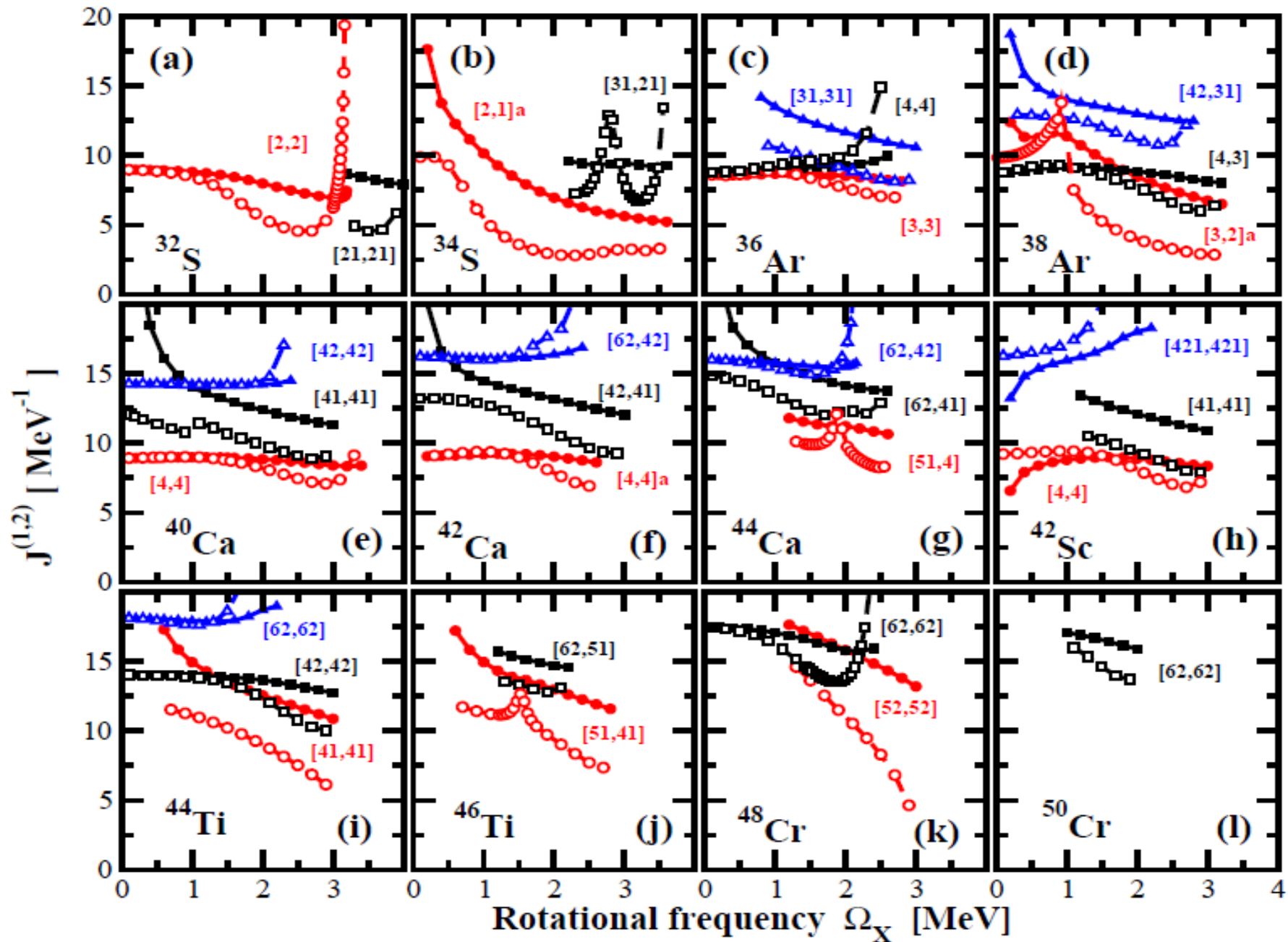
$^{16}\text{O} + ^{12}\text{C} + ^{16}\text{O} ?$



^{36}Ar – the best candidate for observation of HD and MD since the transition to these shapes takes place at $l=18$

$^{16}\text{O} + ^{16}\text{O} + 2n ?$

Kinematic and dynamic moments of inertia



Conclusions

1. Systematic and global investigation of octupole deformed even-even nuclei with an estimate of theoretical uncertainties has been performed for the first time. A new region of octupole deformation, centered around $Z \sim 98$, $N \sim 196$, has been predicted for the first time.

1. Systematic investigation of SHE with an assessment of theoretical uncertainties.
OOPS #1: $N=172$ shell gap is no longer “magic” in CDFT
OOPS #2: $N=184$ shell gap is more important
OOPS #3. $Z=120$ nuclei are not necessary spherical (they may be oblate)

3. Extremely deformed structures inevitably become yrast with increasing spin in the nuclei under study. This is because normal and highly-deformed configurations forming the yrast line at low and medium spins have limited angular momentum content. The nuclei most favored for the observation of extremely deformed structures are located in the vicinity of ^{36}Ar and ^{40}Ca .

4. The $N = Z$ nuclei are better candidates for the observation of extremely deformed structures as compared with the nuclei which have an excess of neutrons over protons since the transition to extremely deformed structures takes place at lower spins.